3D Bioprinting Pancreatic Tumor Spheroids

A Technical Report submitted to the Department of Biomedical Engineering

Presented to the Faculty of the School of Engineering and Applied Science
University of Virginia • Charlottesville, Virginia

In Partial Fulfillment of the Requirements for the Degree
Bachelor of Science, School of Engineering

Ailene Edwards
Spring 2023

On my honor as a University Student, I have neither given nor received unauthorized aid on this assignment as defined by the Honor Guidelines for Thesis-Related Assignments

Advisor Signature:

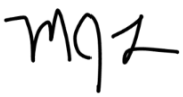

Matthew J. Lazzara

3D Bioprinting Pancreatic Tumor Spheroids

Ailene C. Edwards[a], Matthew J. Lazzara[a,b,1]

[a] University of Virginia, Department of Biomedical Engineering
[b] University of Virginia, Department of Chemical Engineering
[1] Correspondence: mjl9cd@virginia.edu

Abstract

In vivo, cancer cells are exposed to complex signals from surrounding stromal tissue and blood vessel networks. In cancer research, 2D cell culture and 3D spheroid culture models fail to capture the full complexity of the tumor microenvironment because they typically involve single cell types. 3D-bioprinting offers a reproducible and precise method to create patterned tumor spheroids that mimic the intact tumor setting. These models can be used as a platform to interrogate cancer cell phenotypes. Bioprinted constructs were patterned with a core of neoplastic cells surrounded by stromal cell types. To achieve a stable, bioprinted construct, variables such as bioink cooling time and cellular composition were optimized. A 20-minute cooling time at 4°C optimized printability and stability of constructs in the post-print period. We further found that cellular composition affects construct stability, especially in the stromal shell. Incorporation of at least 25% HPAF-II cells in the stromal compartment, along with HUVECs and CAFs, promoted maintenance of an intact stromal shell over a 10-day period. When the stromal shell was printed without HPAF-II cells, the shell was unstable and quickly degraded.

Keywords: Tumor microenvironment, bioprinting, pancreatic cancer models

Introduction

Since 2001, the incidence and mortality of pancreatic cancer has increased[1]. Pancreatic cancer remains one of the deadliest types of cancer, being the fourth leading cause of cancer deaths in the United States[1]. It is associated with a poor prognosis: the five-year survival rate for pancreatic adenocarcinoma is only 10%[2]. Overall, while pancreatic cancer accounts for 3% of all cancer diagnoses, it accounts for 8% of all cancer deaths[1]. Therefore, there is a need to better understand the mechanisms by which pancreatic cancer progresses and to generate improved therapeutic options.

In vivo, pancreatic cancer is influenced by the surrounding environment, referred to as the tumor microenvironment (TME). The TME consists of diverse cell populations, including cancer-associated fibroblasts (CAFs) and immune cells[3]. It is also comprised of extracellular matrix and vascular networks[3]. The heterogenous cell populations and components of the TME affect the progression of pancreatic cancer. For example, fibroblasts may increase invasion via the release of hepatocyte growth factor and mediate chemoresistance[4]. Angiogenesis, or the growth of blood vessel networks, is correlated with rapid tumor progression[4]. Due to the influence of the TME on pancreatic cancer progression, experimental models used to study pancreatic cancer should incorporate elements found in the *in vivo* TME.

There are several limitations of current experimental models of pancreatic. For example, some models fail to faithfully recapitulate the complex environment found inside the human body. Other model types, such as mouse models, represent the TME, but are accompanied by ethical concerns. 2D cell culture fails to incorporate 3D spatial architecture and typically consists of single cell types, leading to inaccuracy in replicating *in vivo* cell behavior[5]. Traditional 3D spheroids are self-assembling cell clusters. 3D spheroids add a spatial dimension over 2D cell culture, but they do not capture the dense stromal tissue commonly surrounding pancreatic cancer cells *in vivo*[6]. Microfluidic systems incorporate characteristics of endothelial networks and stromal tissue, yet may be challenging to scale[6]. Further, such organ-on-a-chip models may affect cell viability[7]. Bioprinting is an emerging technology that offers the opportunity to improve on current experimental models. Bioprinters may spatially pattern cell-laden bioinks and create 3D architecture[8]. 3D-bioprinted cancer models may be designed to better reflect the *in vivo* environment of pancreatic cancer, improving on current experimental models.

Prior research conducted by Langer et al. (2019) from Oregon Health and Sciences University generated a 3D-bioprinted model of cancer[9]. In their approach, an Organovo Novogen MMX bioprinter deposited cell-laden bioink in the spatial pattern of a tumor core, surrounded by a shell of stromal cell types[9]. Fibroblasts and endothelial cells were included in the stromal shell. Fibroblast cell types deposited extracellular matrix, and endothelial cells formed a vascular network in the bioprinted construct[9]. The bioprinted model was used to further interrogate cancer cell phenotypes, including migration and cellular proliferation[9]. Prior to Langer et al., cancer models often included a scaffolding feature[6]. Professor Langer's bioprinted approach was unique in being scaffold-free. The use of a gelatin/alginate hydrogel in the cell-laden bioink allowed for a reversibly crosslinked structure to form in the immediate post-print period for stability[9]. After 48 hours, the crosslinks could be enzymatically degraded by the addition of alginate lyase. The benefit of this approach is that a purely cellular model remains, laid in a spatial pattern that mimics the *in vivo* tumor microenvironment.

Due to the success of Langer et al. in 2019, we proposed a similar protocol and design comprising of a tumor core and stromal shell for the study of pancreatic cancer. At UVA, we have access to different resources and equipment, namely a different bioprinter that must be accounted for in a new protocol. To measure the success of our bioprinted constructs, we considered construct stability, measured based on construct area. The constructs were expected to survive a total of 7-10 days of incubation. Further, we proposed studying distinct populations of CAFs in our bioprinted model to further differentiate from Langer et al.'s work. Prior research has suggested that there are unique types of CAF phenotypes in pancreatic cancer: myofibroblastic and inflammatory fibroblasts[10]. Myofibroblastic CAFs (myCAFs) show elevated expression of the marker αlpha smooth muscle actin (a-SMA) and are located in the immediate area surrounding cancer cells[10]. Inflammatory CAFs (iCAFs) show low expression of α-SMA and high expression of interleukin-6 (IL-6) which is a cytokine[10]. They are located farther from the tumor than myCAFs and exhibit cytokine-secreting properties[10]. We focused on these phenotypes throughout the project.

Results

Bioprinted Model Design

A 3D Discovery bioprinter from RegenHu was used to pattern constructs in a 24-well plate. Constructs were extruded at a pressure of approximately 2 bar, from a 27 gauge needle. The width of the needle affected the height of the construct, as the height of each layer matches the width of the needle. Constructs were printed in three layers. The intended dimensions of the construct were a height of 0.6 mm, a core height of 0.2 mm, an outer shell radius of 1.2 mm, and a core radius of 0.6 mm (Fig 1). The stromal shell is comprised of 0082T CAFs and human umbilical vein endothelial cells (HUVECs). The cancer core is comprised of HPAF-II human pancreatic adenocarcinoma cells. Resulting constructs are cylindrical (Fig 1).

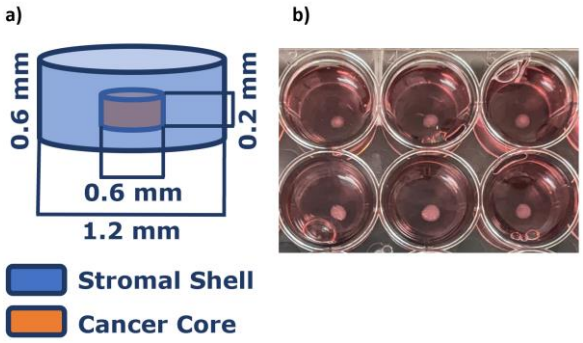

Figure 1: Intended dimensions of bioprinted model (Panel a). Constructs are extruded into a 24-well plate and are incubated in complete media (Panel b).

Early Challenges in Bioprinted Constructs

Bioprinted constructs deviated from intended design and outcomes in early stages. First, in the immediate post-print period, constructs were too runny to maintain the intended shape (Fig 2a). Constructs also degraded throughout the incubation period or upon the addition of alginate lyase at 72 hours post-print (Fig 2b). The stromal shell was more likely to degrade than the cancer core, which sometimes remained densely packed, even when the stromal shell degraded around it (Fig 2c). The bioprinter needles also posed another challenge. When patterning constructs, the needle extruding stromal bioink dragged through the cancer core. This caused the cancer core to be pulled out of its intended circular position, creating lines of cancer cells in the stromal shell (Fig 2d). To correct the displacement of cancer cells by the stromal bioink needle, the printer settings were manipulated. The top layer of the stromal shell was changed to be laid in a circular pattern, rather than a back

and-forth horizontal filling pattern. Further, the needle setting was changed so the stromal bioink needle did not drag through the cancer core layer. These changes affected the attachment of the cancer core. We observed some constructs that showed a cancer core detaching from the stromal shell (Fig 2e). Upon these observations, we reverted to the original settings to prevent further detachment of the HPAF-II compartment of the constructs. We further focused on re-calibrating the needle position as we noted the dragging from the stromal needle may have arisen from mis calibrated needles.

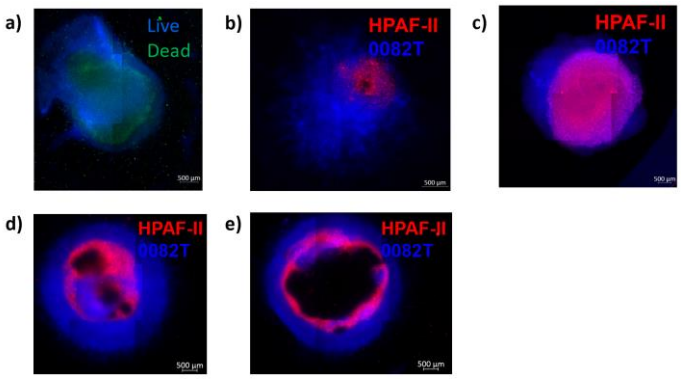

Figure 2: Initial challenges with bioprinted constructs. Constructs were runny and unstable (Panel a). Constructs showed degradation from a densely packed construct (Panel b). In some constructs, the stromal shell degraded away from the cancer core (Panel c). Another challenge was cancer core dragging from the intended printed location by the stromal bioink needle (Panel d). Other constructs showed a cancer core that floated from the construct (Panel e).

Bioink Viscosity

Bioink viscosity was manipulated to improve printability and stability of the constructs. Consistency is a variable of cooling time at 4°C, and we were advised by Professor Langer that ink should extrude without welling at the end of the needle or forming a droplet (Fig 3). Bioink that had been cooled for 25 minutes at 4°C welled at the end of the needle and created constructs that were deformed (Fig 3). Bioink cooled for 10 minutes at 4°C was too runny and led to constructs that did not maintain their shape in the immediate post-print period (Fig 3). Bioink cooled for 20 minutes at 4°C was the most printable, leading to printed constructs that matched the intended design. Further, constructs maintained their shape in the immediate post-print period better than prior results that had created runny constructs. Optimized ink viscosity promoted the stability of constructs through 3 days of incubation, or until the dissolution of the crosslinked alginate structure.

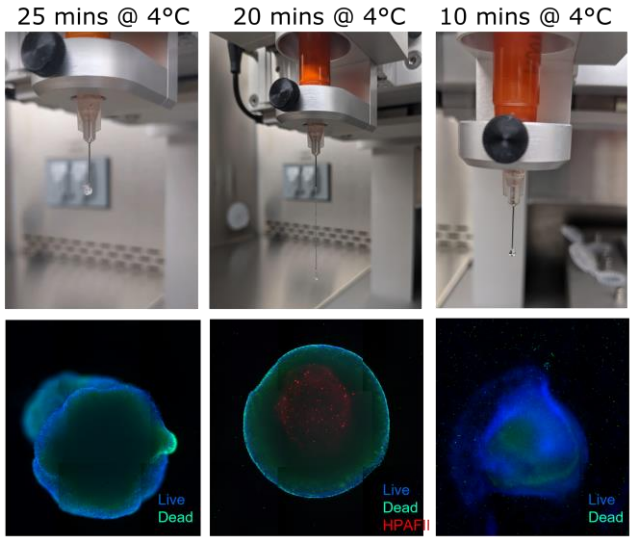

Figure 3: Bioink viscosity and associated construct result. Bioink that has been cooled for 25 minutes at 4°C (left panel). Associated construct does not form desired shape (left panel). Bioink that has been cooled for 20 minutes at 4°C (middle panel). Bioink that has been cooled for 10 minutes at 4°C (right panel). Associated construct is runny and unstable (right panel).

Exogenous Growth Factors

Another avenue that was explored to improve construct stability through 10 days of incubation was the addition of exogenous growth factors to construct media (Fig 4). Transforming growth factor beta (TGF-β) and hepatocyte growth factor (HGF) are growth factors that affect the TME. TGF-β, for example, acts on fibroblast cells to mediate desmoplasia, or the reaction forming a dense stromal tissue surrounding the cancer cells[11]. We hypothesized that the addition of TGF-β to construct media would produce more stable constructs via fibroblast synthesis of extracellular matrix. HGF induces proliferation and migration in cancer cells[12]. We hypothesized that the addition of exogenous growth factors to construct media might induce migration and promote construct stability via the proliferation of cancer cells. Qualitative images of this experiment are shown starting from Day 4, after the dissolution of the alginate crosslinked structure on Day 3 (Fig 4a).

Next, we quantified the percent change in cancer core size (Fig 4b). We observed the cancer core starting on Day 4, after the dissolution of the alginate crosslinked structure and through 10 days of incubation. Cancer core size was used as a metric of cell migration out of the cancer core. Results do not show a significant amount of migration or change in the cancer core size after the addition of exogenous growth factors (Fig 4b). To consider construct stability, we used construct area as a metric. In prior experiments, we

observed the area of the construct decrease as pieces sloughed off the overall construct. Therefore, constructs that maintained their area throughout incubation were more stable. We represented construct area as a percent decrease from Day 0. We computed a percent decrease in size to normalize for differences in initial size. Constructs treated with exogenous growth factors showed improved stability at intermediate time points, but there was not a significant difference at 10 days of incubation (Fig 4c). These results were unexpected. As described previously, we expected to see migration out of the cancer core and improved stability upon the addition of exogenous growth factors.

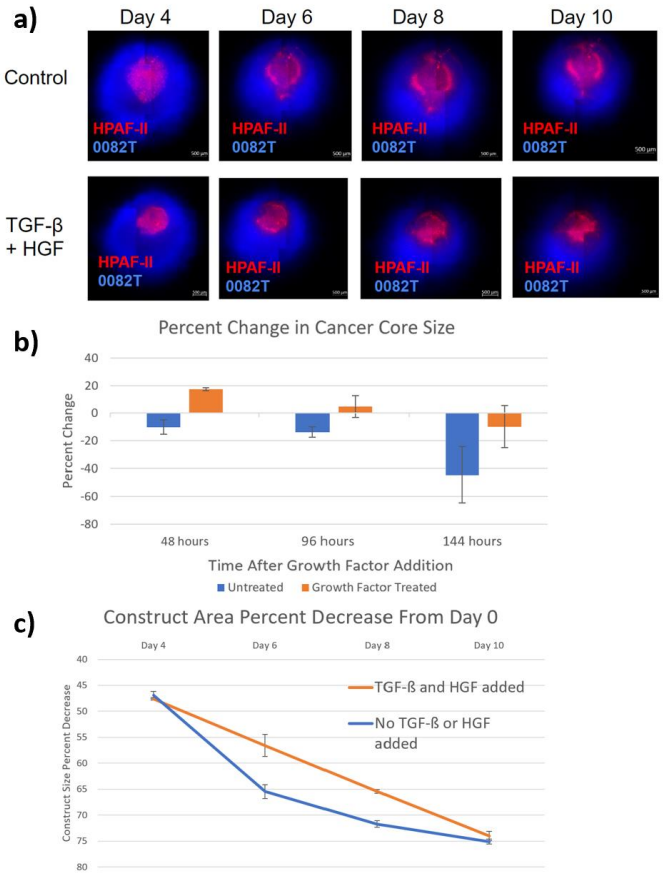

Figure 4: Constructs were incubated with exogenous growth factors through 10 days of incubation (Panel a). Cancer core size was studied as a metric for migration (Panel b). Construct area through 10 days of incubation was measured to represent stability (Panel c) Error bars represent standard error of the mean. For all data points shown, 3 biological replicates were included.

We conducted an immunofluorescence experiment to better understand why constructs incubated with exogenous growth factors may not have shown migration (Fig 5a). We were interested in identifying if the exogenous growth factors had induced the epithelial-to-mesenchymal transition (EMT) in HPAF-II cells. During EMT, cancer cells lose their adherent properties and become more migratory, a phenotype we were interested in studying. We were also interested in identifying if exogenous growth factors had induced a myofibroblastic phenotype in 0082T cells. There were 6 conditions: untreated HPAF-II monoculture, untreated 0082T monoculture, HPAF-II & TGF-β, 0082T & TGF-β, untreated HPAF-II/0082T co-culture, and HPAF-II/0082T co-culture & TGF-β. We probed for vimentin in HPAF-II cells because it is a marker of EMT. In 0082T cells, we probed for α-SMA, a marker of a myofibroblastic phenotype. An early hypothesis was that exogenous growth factors increased a myofibroblastic phenotype in 0082T cells, which limited EMT and migration in HPAF-II cells. Based on this hypothesis, we only included TGF-β into the immunofluorescence experiment as TGF-β affects fibroblast phenotype.

We found that TGF-β alone did not drive a significant increase in vimentin intensity in HPAF-II monoculture ($p = 0.2574$) (Fig 5b). However, co-culturing HPAF-II with

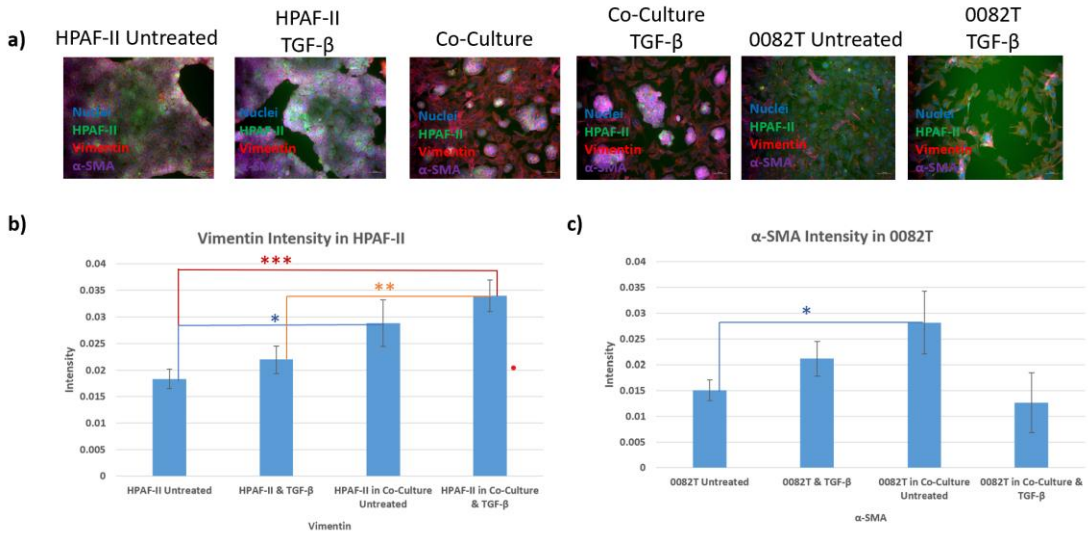

Figure 5: Immunofluorescence experiment with 6 conditions (Panel a). HPAF-II cells were probed for vimentin intensity while 0082T cells were probed for α-SMA intensity. Vimentin intensity per HPAF-II cell in each condition was measured (Panel b). α-SMA intensity per 0082t cell was measured (Panel c). *, **, *** indicate statistical significance between results, calculated using an unpaired t-test. Error bars represent standard error of the mean. For all data points shown, 3 biological replicates were included.

0082T cells did drive a significant increase in HPAF-II vimentin intensity over HPAF-II monoculture ($p = 0.0296$). This was also the case for TGF-β treated conditions. There was an increase in HPAF-II vimentin intensity in treated HPAF-II/0082T co-culture over treated HPAF-II monoculture ($p = 0.002$) (Fig 5B). HPAF-II cultured in proximity to 0082T cells most closely represented a bioprinted construct condition. There was not a significant difference between the treated and untreated co-culture conditions ($p = 0.286$). This is a possible mechanism for why migration may not have been shown when exogenous growth factors were added to constructs: the TGF-β did not induce a significant increase in vimentin intensity between co-cultured conditions. Migration would be more likely to be driven by proximity of HPAF-II cells to 0082T cells, as shown in the influence of co-cultured conditions. In both constructs studied for migration, HPAF-II/0082T were proximal due to construct design.

TGF-β alone did not increase α-SMA expression in 0082T monoculture cells ($p = 0.1176$) (Fig 5c). However, co-culturing 0082T and HPAF-II cells did increase α-SMA expression ($p = 0.0418$) (Fig 5c). There was not a significant difference between the treated vs. untreated co-culturing condition ($p = 0.0662$). Again, the treated co-culture condition most closely represents the bioprinted constructs. Therefore, treating constructs with TGF-β does not significantly elevate a myofibroblastic phenotype. Rather, data suggest the proximal placement of HPAF-II and 0082T cells in the construct does so. These results show that exogenous growth factors alone may not influence construct behavior. Rather, much of construct behavior would arise from HPAF-II/0082T proximity.

Construct Cellular Composition

Prior observations indicated that the cancer core often remained stable and intact, even if the stromal shell deteriorated (Fig 2c). Based on these observations, we hypothesized that HPAF-II cells may contribute to stability. We decided to include a percentage of HPAF-II into the stromal shell compartment to further improve construct stability. Constructs that included 25% HPAF-II in the stromal shell survived standard culture conditions through 10 days of incubation (Fig 6a). Prior constructs had survived the dissolution of alginate lyase but often failed to last for 10 days. As with the exogenous growth factors experiment, we quantified construct stability using construct percent area decrease from Day 0 (Fig 6b). Including 25% HPAF-II in the stromal shell improved construct stability at intermediate time points and through 10 days of incubation.

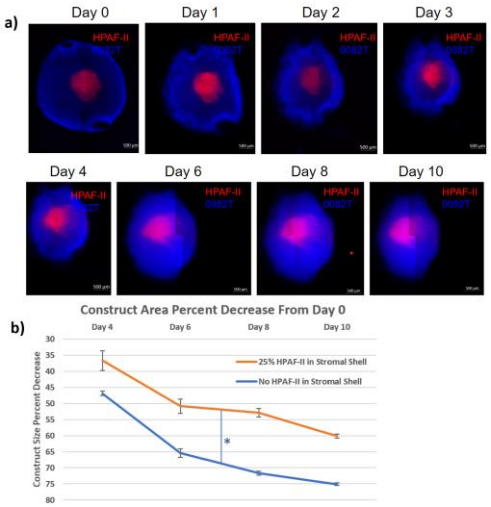

Figure 6: Constructs were bioprinted with 25% HPAF-II included in the stromal bioink (Panel a). Stability of constructs with 25% HPAF-II included in the stromal shell was measured (Panel b). Error bars represent standard error of the mean. For all data points shown, 3 biological replicates were included. Asterisk refers to statistical significance between the two conditions.

Next, we were interested in interrogating the biological basis for the results seen when including 25% HPAF-II into the stromal shell. We conducted a 2D immunofluorescence experiment including 3 conditions: 0082T monoculture, 0082T monoculture cultured with TGF-β as a positive control, and a coculture, including 0082T and HPAF-II cells (Fig 7a). The markers of interest were α-SMA and IL-6. We found 0082T cells in HPAF-II coculture show elevated expression of α-SMA ($p=0.004$) (Fig 7b). There was no significant difference in IL-6 expression across conditions

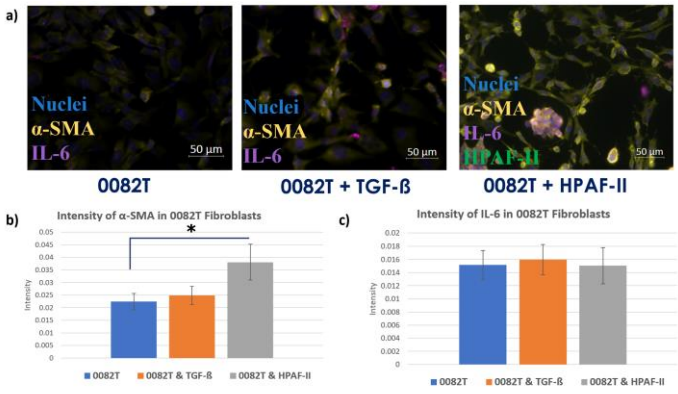

Figure 7: Immunofluorescence experiment with 3 conditions: 0082T monoculture, 0082T monoculture treated with TGF-β, and 0082T/HPAF-II co-culture with HPAF-II comprising 25% total cells (Panel a). Intensity of α-SMA per cell in the 3 experimental conditions is shown (Panel b). These results were calculated using a one-way ANOVA test followed by Tukey's HSD test. Asterisk refers to statistical significance between the three conditions. Intensity of IL-6 per cell in the 3 experimental conditions is shown (Panel c). Error bars represent standard error of the mean. For all data points shown, 3 biological replicates were included.

(p=0.1196) (Fig 7c). The elevated expression of α-SMA suggests that 0082T fibroblasts gain a myofibroblastic phenotype when 25% HPAF-II cells are included in the stromal bioink. Myofibroblastic cells may deposit extracellular matrix that contributes to construct stability.

Discussion

To generate a biologically mimetic model of pancreatic cancer, we leveraged bioprinting technology to spatially pattern cell-laden bioinks. The pattern consisted of a cancer-core and a stromal-shell. We intended for the model to survive through 7-10 days of incubation and exhibit phenotypes characteristic of pancreatic cancer, including cell migration and proliferation. During the bioprinting process, we dissolved the crosslinked alginate structure on Day 3, leaving a purely cellular model. Bioprinting represents one method of approaching improved pancreatic cancer models. We adapted our protocol from Langer et al., 2019[9].

We determined the main influence on cellular behavior within constructs was due to proximal placement of HPAF-II and 0082T cells. Further, adding 25% HPAF-II into the stromal bioink improved construct stability. These results may be linked to a myofibroblastic 0082T phenotype, represented by elevated α-SMA intensity. Constructs remained stable through 10 days of incubation at 37°C and 5% O_2.

Remaining Challenges

While we were successful in manufacturing stable constructs, there remain several shortcomings in the current protocol. First, the overall bioprinting success rate is low. The protocol is inconsistent and is not robust enough to be implemented as a standard model. During the bioprinting process, pressure may need to be adjusted or the bioink yield may vary. This introduces variables into the bioprinting process that must be addressed as they arise. In addition, for each bioprinting experiment, a significant amount of cells are needed. The 3D Discovery RegenHu uses a 3 mL cartridge, causing a larger amount of dead volume. At least 0.2 mL of bioink, at a density of 1.5×10^8 cells/mL is required. To reach this quantity, approximately 4-5 15 cm cell culture plates are required. Overall, the current bioprinting protocol must be adapted to improve consistency. A potential future avenue includes using a piston-based extrusion bioprinter rather than pneumatic-based. A pneumatic-based bioprinter uses air pressure that may not displace bioink as precisely as a piston-based bioprinter, affecting resolution[13]. Another potential future avenue includes bioprinting into matrix material to reduce the likelihood of construct degradation or collapse over time.

Further, another remaining challenge is that many standardized methods of studying cells were created for 2D models. For example, to understand the results of increased stability in constructs or a lack of migration, we turned to 2D immunofluorescence. A future direction for this project is to adapt methods to study constructs, beyond ImageJ analysis. Bioprinted constructs may need to be cross sectioned to better study markers and cellular dynamics within the 3D model. Professor Langer used methods such as a cancer cell closeness centrality score (CCS) to study migration. Langer et al. also used CD31+ staining, trichrome staining, and immunofluorescence[9]. These methods were used to visualize a vascular network in the construct, view collagen as a metric of extracellular deposition, and to study cell markers.

Materials and Methods

Cell Culture

All cells were maintained in a cell culture incubator at 37°C and 5% CO_2. Human pancreatic adenocarcinoma cells (HPAF-II) were cultured in RPMI (Thermo Fisher Scientific) supplemented with 10% FBS, 2% penicillin/streptomycin, and 2% L-glutamine. 0082T CAFs were cultured in DMEM (Thermo Fisher Scientific) supplemented with 10% FBS, 2% penicillin/streptomycin, and 2% L-glutamine. Human umbilical vein endothelial cells (HUVECs) were purchased from Millipore Sigma (SCCE001) and were cultured using PeproGrow MacroV Media (Peprotech) and EGM-2 Endothelial Cell Growth Medium with EBM-2 supplements (Lonza). Cells were cultured to 80% confluence in 10 cm and 15 cm TC plastic dishes. HPAF-II and 0082T cells were maintained under passage 20, while HUVEC cells were maintained between passage 3-6. HPAF-II cells were stained with DiI Cell-Labeling Solution (Thermo Fisher Scientific) for visualization. Cells were mixed into hydrogel at a density of 1.5×10^8 cells/mL of bioink.

Bioprinting Reagents and Equipment

The protocol is based heavily on Professor Ellen Langer's approach derived from discussions with her and from her 2019 *Cell Reports* paper[9]. Our protocol differs in the type of bioprinter used and the type of fibroblast line included. Further, we included a wash step after the addition of

calcium chloride and did not print into transwell membranes.

Gelatin from porcine skin, Type A (Sigma-Aldrich) and Alginic Acid Sodium Salt (Sigma-Aldrich) were mixed into DPBS (Thermo Fisher Scientific) to form a hydrogel comprised of 6% w/v gelatin and 1% w/v alginate. Cells are mixed into a gelatin-alginate bioink at a density of 1.5 x 10^8 cells/mL of ink. Cell laden bioinks were placed in 3 mL UV-shielding cartridges (Cellink) and were extruded through 27G 0.5" 0.2 mm needles (Cellink). Constructs were manufactured using a 3D Discovery Printer (RegenHu, Switzerland). Extrusion pressure may be manually adjusted. Bioprints occurred at a pressure of 2 bar for both the cancer and stromal cartridge. They were designed using BioCAD (RegenHu) software. Extruded constructs were treated with a 2% calcium chloride (Sigma-Aldrich) solution to reversibly crosslink the sodium alginate. Constructs were washed once with 2 mL DPBS (Thermo Fisher Scientific) and incubated at 37°C and 5% CO_2 in media consisting of equal parts of each cell media needed. Constructs were stained with NucBlue Live Ready Probe Kit Reagent (Thermo Fisher Scientific) immediately after printing. NucBlue stain was added at a concentration of 2 drops/mL as described in product manual. After 3 days of incubation, alginate lyase (Sigma-Aldrich) was added at a concentration of 0.2 mg/mL of media.

2-D Immunofluorescence

Cells were seeded onto coverslips in 6-well plates. Cell lines included in immunofluorescence experiments were HPAF-II and 0082T. Upon reaching desired confluence, cells were washed with 3 mL DPBS (Thermo Fisher Scientific). 4% paraformaldehyde (Thermo Fisher Scientific) in DPBS was used to fix cells for 20 minutes. Wells were washed twice with DPBS. 0.25% Triton-X 100 in DPBS was used to permeabilize cells for 5 minutes, followed by 2 DPBS washes. Primary antibody (R&D Systems AF-206-NA, Santa Cruz SC 32251, Cell Signaling Technology CST #5741S) was prepared in Intercept Blocking Buffer (Li-Cor). Plates were incubated at 37°C for 3 hours. Coverslips were washed with PBS-Tween (Thermo Fisher Scientific). Secondary antibody (Alexa fluor 647 goat anti-mouse, Thermo Fisher Scientific A32728, Alexa fluor 647 donkey antigoat, Thermo Fisher Scientific A21447, Alexa Fluor 546 goat anti-rabbit, Thermo Fisher Scientific A11035) was prepared in Intercept Blocking Bugger. Prolong Gold Antifade (Thermo Fisher Scientific) was used to mount coverslips on imaging slides. Images were captured at 20x on a Zeiss Axiovert Z1 microscope. CellProfiler software was used to quantify marker intensity per cell from images.

Imaging and Growth Factors

Tiled images were captured using a Zeiss Axiovert Z1 Microscope. To perturb the construct, growth factors were added upon the dissolution of the alginate crosslinked structure at 3 days post-print. Recombinant human TGF-β1 and HGF (Peprotech) were added at concentrations of 10 and 50 ng/mL, respectively. Media changes occurred every 48 hours, with refreshed media and growth factors added to construct wells. ImageJ software was used to measure construct area from tiled czi images.

Statistical Analysis

Statistical analysis was conducted in Excel software. ANOVA followed by Tukey's HSD was used to compare data from three-condition immunofluorescence experiments. Unpaired t-tests were used to compare pairs of conditions in larger immunofluorescence experiments.

End Matter

Author Contributions and Notes

A.E. and M.L. designed research, A.E performed research, analyzed data, and wrote the paper.

The authors declare no conflict of interest.

Acknowledgments

I would like to thank Professor Matthew Lazzara, PhD for his sponsorship of this capstone research study. I would also like to thank members of the UVA Lazzara Lab, Peirce-Cottler Lab, and Highley Lab for their consistent support and guidance. Further, I would like to thank Professor Ellen Langer from the Oregon Health and Science University for her advice. Lastly, I would like to thank UVA CADBio Center for Advanced Biomanufacturing and the UVA Office of Undergraduate Research (Harrison Undergraduate Research Award) for their funding support.

References

1. Nierengarten, M. B. Annual report to the nation on the status of cancer. *Cancer* **129**, 8–8 (2023).
2. Osuna de la Peña, D. *et al.* Bioengineered 3D models of human pancreatic cancer recapitulate in vivo tumour biology. *Nat. Commun.* **12**, 5623 (2021).
3. Murakami, T. *et al.* Role of the tumor microenvironment in pancreatic cancer. *Ann. Gastroenterol. Surg.* **3**, 130–137 (2019).
4. Farrow, B., Albo, D. & Berger, D. H. The Role of the Tumor Microenvironment in the Progression of Pancreatic Cancer. *J. Surg. Res.* **149**, 319–328 (2008).

5. Jensen, C. & Teng, Y. Is It Time to Start Transitioning From 2D to 3D Cell Culture? *Front. Mol. Biosci.* **7**, (2020).
6. Tomás-Bort, E., Kieler, M., Sharma, S., Candido, J. B. & Loessner, D. 3D approaches to model the tumor microenvironment of pancreatic cancer. *Theranostics* **10**, 5074–5089 (2020).
7. Terrell, J., Jones, C., Monia Kabandana, G. K. & Chen, C. From cells-on-a-chip to organs-on-a-chip: scaffolding materials for 3D cell culture in microfluidics. *J. Mater. Chem. B* **8**, 6667–6685 (2020).
8. Neufeld, L., Yeini, E., Pozzi, S. & Satchi-Fainaro, R. 3D bioprinted cancer models: from basic biology to drug development. *Nat. Rev. Cancer* 1–14 (2022) doi:10.1038/s41568-022-00514-w.
9. Langer, E. M. *et al.* Modeling Tumor Phenotypes In Vitro with Three-Dimensional Bioprinting. *Cell Rep.* **26**, 608-623.e6 (2019).
10. Öhlund, D. *et al.* Distinct populations of inflammatory fibroblasts and myofibroblasts in pancreatic cancer. *J. Exp. Med.* **214**, 579–596 (2017).
11. Watt, D. M. & Morton, J. P. Heterogeneity in Pancreatic Cancer Fibroblasts—TGFβ as a Master Regulator? *Cancers* **13**, 4984 (2021).
12. Pothula, S. P. *et al.* Targeting the HGF/c-MET pathway: stromal remodelling in pancreatic cancer. *Oncotarget* **8**, 76722–76739 (2017).
13. Kačarević, Ž. P. *et al.* An Introduction to 3D Bioprinting: Possibilities, Challenges and Future Aspects. *Materials* **11**, 2199 (2018).